Heliyon 8 (2022) e09100

Contents lists available at ScienceDirect

Heliyon

journal homepage: www.cell.com/heliyon

Research article

Enhanced circulation longevity and pharmacodynamics of metformin from surface-modified nanostructured lipid carriers based on solidified reverse micellar solutions☆

Franklin Chimaobi Kenechukwu *, God'spower Tochukwu Isaac, Daniel Okwudili Nnamani, Mumuni Audu Momoh, Anthony Amaechi Attama

Drug Delivery and Nanomedicines Research Group, Department of Pharmaceutics, Faculty of Pharmaceutical Sciences, University of Nigeria, Nsukka 410001, Enugu State, Nigeria

ARTICLE INFO

Keywords:
PEGylated nanostructured lipid carrier (NLC)
Solidified reverse micellar solution (SRMS)
Metformin
Beeswax
Anti-diabetic activity
Phospholipon ® 90H

ABSTRACT

Metformin hydrochloride (MTH) has been associated with poor/incomplete absorption (50–60%), low bioavailability, short half-life (0.4–0.5 h), high dosage and dose-related side effects. To overcome these barriers and improve oral bioavailability and efficacy of MTH, surface-modified nanostructured lipid carriers (NLCs) were developed. Lipid matrices composed of rational blends of beeswax and Phospholipon® 90H (as solid lipids) and Capryol-PGE 860 (as liquid lipid) were prepared by fusion, and the resultant lipid matrices were PEGylated to give 10, 20 and 40% PEGylated lipid matrices. MTH-loaded non-PEGylated and PEGylated NLCs were prepared via high-shear hot homogenization and characterized regarding particle properties and physicochemical performance. The encapsulation efficiencies (EE%) and loading capacities (LC) of the MTH-loaded NLCs were determined while the *in vitro* drug release was evaluated in phosphate buffered saline (PBS, pH 7.4). Antidiabetic and pharmacokinetics properties of the NLCs were ascertained in an alloxan-induced diabetic rats model after oral administration. The MTH-loaded NLCs were nanomeric (particle size: 184.8–882.50 nm) with low polydispersity index (0.368–0.687) and zeta potential (26.5–34.2 mV), irregular shape, amorphous nature with reduced crystallinity. The EE% and LC were >90 % and 16%, respectively. The formulations showed >65 % release over 12 h in a greater sustained manner than marketed MTH formulation (Glucophage®) as well as enhanced pharmacokinetics properties and sustained blood glucose lowering effect, even at reduced doses with PEGylated NLCs than Glucophage®. Thus, PEGylated NLC is a promising approach for improved delivery and oral bioavailability of MTH thus encouraging further development of the formulation.

1. Introduction

Metformin is a widely prescribed antidiabetic drug [1], belonging to the class III biopharmaceutics classification system (BCS), characterized by high solubility and low permeability [2], which lowers basal and postprandial blood glucose concentrations. In recent treatment guidelines for diabetes management issued by the American Diabetes Association and European Association for the Study of Diabetes, metformin is indicated as the first-line pharmacotherapeutic agent for the treatment of type 2 diabetes mellitus [1]. Despite its wide usage, upon oral administration, metformin is known to be associated with low and incomplete gastrointestinal absorption (40–60 %), comparatively high pre-systemic clearance – resulting into low bioavailability, and relatively short biological half-life (0.4–0.5 h). These pharmacokinetic properties of metformin culminate into high dose administrations and dosage frequency, increased incidence of dose-related side effects, and reduced patients' compliance [3, 4, 5]. As measures which provide certain levels of solutions and improvements, formulation and biomaterial scientists have designed, developed and explored several novel delivery systems with modifications through chemical and physical methods [5]. Amongst these measures are lipid drug delivery systems (solid lipid microparticles, lipid-drug conjugates, solid lipid nanoparticles, nanostructured lipid carriers, etc.) and surface modification (such as PEGylation) or functionalization.

☆ This article is a part of the "Lipid-Based Nanoparticles" Special issue.

* Corresponding author.
E-mail addresses: frankline.kenechukwu@unn.edu.ng, chimafrankduff@yahoo.com (F.C. Kenechukwu).

https://doi.org/10.1016/j.heliyon.2022.e09100
Received 19 August 2021; Received in revised form 9 November 2021; Accepted 9 March 2022
2405-8440/© 2022 The Author(s). Published by Elsevier Ltd. This is an open access article under the CC BY-NC-ND license (http://creativecommons.org/licenses/by-nc-nd/4.0/).

This study investigated the pharmacodynamic effects of metformin delivered orally through a surface modified-lipid-based drug delivery system – PEGylated nanostructured lipid carriers (NLCs). NLCs are nano-delivery systems made up of rational mix of solid lipids with spatially incompatible liquid/fluid lipids, preferably in ratios of 70:30 to 99.9:0.1, presenting as imperfect-type, amorphous-type or multiple-type NLC. NLC was developed as a result of the search by formulation scientists for the solutions to the failures/limitations of solid lipid nanoparticles (SLNs) and other colloidal carriers viz., nanoemulsion, polymeric nanoparticles, liposomes, etc. Such limitations, including low payload, drug expulsion during storage, and high water content, have been surmounted by the whole set of unique advantages of NLCs [6]. These advantages include enhanced drug loading capacity, prevention of drug expulsion, improved flexibility for drug release, and versatility for various routes of administrations. Also, NLC matrices accommodate more drug molecules than solid lipid nanoparticles. This is due to the special spatial arrangements of different lipid molecules – liquid and solid lipids – within NLC matrix, which increases the imperfection of the matrix, thus allowing NLCs to load more drug molecules [7, 8].

Nanoparticles are known to possess chemical and physical properties which affect their pharmacokinetics and biodistribution. The size, surface charge and surface chemistry of nanoparticles affect their intracellular uptake and internalization, and this also culminates into increased serum protein (opsonins) binding through a process called opsonization and the resultant uptake and internalization by macrophage - also called reticuloendothelial system (RES) or the mononuclear phagocytes system (MPS) [9]. Hence, nanoparticles and the drug molecules loaded in them are lost from the circulation. To improve the plasma circulation time of nanoparticles and prevent unnecessary drug loss, formulation scientists employ the methods of nanoparticle surface modification and/or functionalization [10]. One of the most popular methods of nanocarriers-surface modification is PEGylation [9].

PEGylation is a process that involves the use of polyethylene glycol (PEG), a non-toxic, non-irritant, inert hydrophilic polymer, which is conjugated on the surface of the nanoparticles by covalent grafting, entrapping or adsorbing of PEG chain [5, 10]. The PEG chains provide steric hindrances against plasma protein binding; thus, improve the stability of nano-drug delivery systems. The resultant effect is improved pharmacokinetics and pharmacodynamics of nanoparticles and drugs, improved biodistribution and dwelling time at the site of action, and increased therapeutic efficacy due to increased drug concentration. PEGylation has made possible the optimized delivery of both hydrophilic and hydrophobic drugs [5, 9, 11].

Metformin is a hydrophilic drug, always recommended to be administered orally with food to improve its absorption and bioavailability. A clinical trial conducted to determine the effect of food on the pharmacokinetics of metformin has proven that the bioavailability of metformin is significantly increased when administered with fatty meal [12]. This informed our choice of lipid-based delivery system as our proposed potential carrier for enhanced delivery of metformin. Over the years, formulation scientists have employed NLCs as novel lipid-based delivery vehicle for therapeutic molecules – including hydrophobic and hydrophilic drug molecules [13] – thus achieving smart, targeted, controlled and/or sustained drug release for improved efficacy/potency [14, 15, 16, 17]. More so, PEGylation has also proven to be an effective means of enhancing the properties of NLCs in the delivery of drugs [18, 19, 20, 21, 22, 23]. More recently, a comparative study carried out by *Qushawy* [2] involved the use of Capryol 90-based NLC to investigate optimization of formulations for controlled release of metformin and enhanced metformin penetration. However, the paucity of information in the literature on the potential merits of using PEGylated Capryol-polyglycerol ester (PGE) 860-based NLCs based on beeswax for the delivery of metformin necessitated this investigation. Capryol-PGE 860 (propylene glycol monocaprylate), a monoester of caprylic acid, is semi-synthetic oil which is used as the liquid lipid for the preparation of the NLC lipid matrices. It has self-emulsifying properties, bioavailability-enhancing properties due to its inhibitory actions on CYP3A4 enzyme, as well as prevents agglomeration in formulations [24]. The significance is that PEGylated NLC would impart a lipophilic character to the hydrophilic metformin, this will help better membrane permeability thereby increasing its antidiabetic efficacy and oral bioavailability. This technique has been used to enhance the therapeutic efficacy of drugs by enabling increased drug concentration and longer dwelling time at the site of action via various routes [20, 21, 22, 23]. The novelty embodied in this research is that this is the first report on the use of PEGylated NLCs based on solidified reverse micellar solutions (SRMS) of beeswax and Phospholipon® 90H (a phospholipid) template with Capryol-PGE 860 for enhanced antidiabetic activity and oral bioavailability of metformin. The NLCs formulated were characterized based on morphology, thermal properties, compatibility studies, particle sizes, and polydispersity indices. Also, the encapsulation efficiency (EE %) and *in vitro* drug release patterns of the NLCs were evaluated. Furthermore, the *in vivo* pharmacodynamic (antidiabetic) properties of the NLC formulations were evaluated using alloxan-induced diabetic animal model, in comparison with a commercial metformin sample (Glucophage®).

2. Materials and methods

2.1. Materials

The pure sample of metformin used was obtained as a gift from May and Baker PLC (Ikeja, Lagos State, Nigeria). Phospholipon® 90H (P90H) (Phospholipid GmbH, Köln, Germany), sorbitol (Caesar & Loretz, Hilden, Germany), sorbic acid (Foodchem Int. Co., China), polyethylene glycol 4000 (PEG 4000) (Ph. Eur. Carl Roth GmbH + Co. KG Karlsruhe, Germany), beeswax (Carl Roth, Karlsruhe, Germany), Polysorbate 80 (Tween® 80) (Acros Organics, Geel, Belgium), Capryol-PGE 860 (Gattefossé, Saint – Priest Cedex, France), Glucophage® purchased from model pharmacy University of Nigeria, Nsukka (Merck KGaA, Darmstadt, Germany), Alloxan (Merck KGaA, Darmstadt, Germany) and double distilled water (Lion water, University of Nigeria, Nsukka, Nigeria) and other solvents and reagents were used as procured from their manufacturers without further purification. Adult albino Wistar rats of both sexes were procured from the Faculty of Veterinary Medicine, University of Nigeria, Nsukka, Nigeria.

2.2. Methods

2.2.1. Preparation of non-PEGylated and PEGylated lipid matrices

Non-PEGylated and PEGylated lipid matrices were prepared by fusion method [25] using beeswax (BW) and Phospholipon® 90H (P90H) (as solid lipids) in combination with Capryol-PGE 860 (as liquid lipid) followed by PEGylation. The solid lipids and liquid lipid were used at 7:3 ratio (i.e. 21.0 g of BW/P90H admixture and 9.0 g of capryol-PGE 860). First of all, the solid lipids (21.0 g of beeswax and 9.0 g of P90H) were weighed, added in a glass beaker placed in an oil bath (liquid paraffin) and melted together in the temperature-regulated bath at a temperature of 70 °C. The combination mixture was vigorously mixed consistently until a transparent white melt which was homogenous was obtained. The homogenous mixture of the lipid matrix (LM_1) was mixed further at room temperature until it solidifies. This lipid matrix (LM_1) was melted after 24 h in a thermo-controlled bath at a temperature of 80 °C followed by addition of the liquid lipid [9.0 g or 8.98 ml of capryol-PGE 860]. The mixture was stirred further to get a homogenous, transparent white melt [lipid matrix (LM_3)] which was allowed to solidify also at room temperature. Moreso, after 24 h, various quantities (90, 80 and 60 %w/w) of the latest prepared non-PEGylated lipid matrix (LM_3) were melted together with corresponding amounts of polyethylene glycol (PEG 4000)

(10, 20 and 40 %w/w) incorporated at 80 °C over the oil bath to give PEGylated lipid matrices (PEG-LM_1, PEG-LM_2 and PEG-LM_3) containing 1:9, 2:8, 4:6 ratios of PEG: lipid matrix, respectively, which were stirred properly and allowed to solidify also. The non-PEGylated and PEGylated lipid matrices were thereafter stored in airtight and moisture resistant glass bottles away from light until used.

2.2.2. Preparation of drug-loaded non-PEGylated and PEGylated lipid matrices

Representative drug-loaded non-PEGylated and PEGylated lipid matrices were prepared by fusion [14] using the non-PEGylated and PEGylated lipid matrices and metformin. With target non-PEGylated and PEGylated lipid concentration of 5.0 %w/w and target drug concentrations of 1.0 %w/w of metformin in the non-PEGylated and PEGylated nanostructured lipid carriers to be developed, 2.5 g of each of the lipid matrices was melted in the temperature-regulated oil bath at a temperature of 80 °C followed by addition of 0.5 g of metformin. Each of the mixture was stirred continuously until a homogenous, transparent white melt was obtained. The homogenous mixtures of the drug-loaded lipid matrices (MTH-loaded LM_3 and MTH-loaded PEG-LM_3 or Drug-loaded LM_3 and Drug-loaded PEG-LM_3) were stirred further at room temperature, allowed to solidify and thereafter stored in airtight and moisture resistant glass bottle in the refrigerator until used.

2.2.3. Differential scanning calorimetry (DSC) analysis of plain and drug-loaded lipid matrices

Thermal properties of beeswax, Phospholipon® 90H (P90H), beeswax-based P90H-modified lipid matrix (LM_1), capryol-containing non-PEGylated beeswax-based P90H-modified lipid matrix (LM_3), PEG 4000, capryol-containing PEGylated beeswax-based P90H-modified lipid matrix (PEG-LM_3), metformin and metformin-loaded non-PEGylated and PEGylated beeswax-based P90H-modified lipid matrices (MT-loaded LM_3 and MT-loaded PEG-LM_3 or Drug-loaded LM_3 and Drug-loaded PEG-LM_3) were determined using a differential scanning calorimeter (DSC Q100 TA Instrument, Germany). About 5 mg of each sample was weighed into an aluminum pan, hermetically sealed and the thermal behavior ascertained in the range of 20–350 °C at a heating rate of 5 °C/min. The temperature was maintained at 80 °C for 10 min and thereafter, cooled at the rate of 5–10 °C/min. Before the determinations, baselines were determined using an empty pan, and all the thermograms were baseline-corrected.

2.2.4. Fourier transform infra-red (FT-IR) spectroscopic analysis of drug-loaded lipid matrices

The spectroscopic analysis was conducted on metformin and representative metformin-loaded capryol-containing non-PEGylated and PEGylated beeswax-based P90H-modified lipid matrices (MTH-loaded LM_3 and MTH-loaded PEG-LM_3 or Drug-loaded LM_3 and Drug-loaded PEG-LM_3) using a Shimadzu FT-IR 8300 Spectrophotometer (Shimadzu, Tokyo, Japan) at the wavelength region of 4000 to 400 cm^{-1} with threshold of 1.303, sensitivity of 50 and resolution of 2 cm^{-1} range. Data collection was done using a smart attenuated total reflection (SATR) accessory. Approximately 0.1 g of each sample was mixed with 0.1 ml nujul diluent. The solution was introduced into the potassium bromate (KBr) plate, which was initially cleaned with a tri-solvent (acetone–toluene–methanol at 3:1:1 ratio) mixture for baseline scanning, and compressed into discs by applying a pressure of 5 tons for 5 min in a hydraulic press. The pellets were placed in the light path and spectra collected in 60 s using Gram A1 spectroscopy software, and the chemometrics were performed using TQ Analyzer1.

The above procedure was extended to the determination of the compatibility of non-PEGylated and PEGylated NLC formulations by FT-IR spectroscopy. However, in this case, approximately 0.1 ml volume of each of the formulation was mixed with 0.1 ml nujul diluent, introduced into the KBr plate before compression into discs.

2.2.5. Preparation of non-PEGylated and PEGylated nanostructured lipid carriers

Non-PEGylated and PEGylated nanostructured lipid carriers encapsulating metformin (G_0, G_{10}, G_{20}, G_{40}) were prepared using the drug, non-PEGylated and PEGylated lipid matrices, Polysorbate® 80 (Tween® 80) (mobile surfactant), sorbitol (cryoprotectant) and distilled water (vehicle) by the high shear hot homogenization method [7, 14, 25, 26]. Briefly, specified quantity of each of the lipid matrix (5 %w/w) was placed in glass beaker and melted at 80 °C in the temperature-regulated heater (IKA instrument) and the drug (1.0 %w/w of metformin) was added to the melted lipid matrix. At the same time, an aqueous surfactant solution consisting of sorbitol (4 %w/w) and Polysorbate® 80 (2 %w/w) was prepared in a separate beaker and heated at the same temperature. The hot aqueous surfactant phase was then dispersed in the hot lipid phase (oily phase) using a high speed homogenizer (Ultra-Turrax T25, IKA-Werke, Staufen, Germany) at 1000 rpm for 5 min. The resulting pre-emulsion was homogenized at 15,000 rpm for 30 min, and allowed to cool properly at room temperature. In this manner, non-PEGylated lipid matrix (LM_3), as well as PEGylated lipid matrices (PEG-LM_1, PEG-LM_2 and PEG-LM_3) were used to prepare non-PEGylated NLC (G_0) as well as PEGylated NLC (G_{10}, G_{20}, and G_{40}), respectively. The formulation compositions of the non-PEGylated and PEGylated NLCs are shown in Table 1.

2.3. Characterization of non-PEGylated and PEGylated NLCs

2.3.1. Determination of particle sizes, polydispersity indices and surface charges

The particle properties [average particle diameter, Z. Ave (nm) and polydispersity indices (PDI)] of the formulations were measured using a zetasizer nano-ZS (Malvern Instrument, Worceshtire, UK) equipped with a 10 mw He-NE laser employing the wavelength of 633 nm and a back-scattering angle of 173^0 at 25 °C. Prior to the photon correlation spectroscopic (PCS) analysis, each sample was diluted with double-distilled water to obtain a suitable scattering intensity.

Zeta potentials or surface charges (ζ) of metformin-loaded PEGylated and metformin-loaded non-PEGylated nano lipid carrier formulations were estimated using dynamic light scattering (DLS) (Malvern Instruments, Japan). In each case, samples were diluted with deionized water) to avoid multiple scattering and to maintain the number of counts per second in the region of 600, and measured at angle of 90° and temperature of 25 °C. All measurements were performed in triplicate and averaged.

2.3.2. Scanning electron microscopy (SEM)

The morphological characteristics of the formulations (representative batch) were determined by a scanning electron microscope (JEOL-JSM-6 360, Japan) at different magnifications. One drop of sample was placed on a slide and excess water was left to dry at room temperature. The slide was attached to the specimen holder using double coated adhesive tape and gold coating under vacuum using a sputter coater (Model JFC-1100, JEOL, Japan) for 10 min, and then investigated at 20 kV.

2.3.3. Determination of encapsulation efficiency (EE %) and loading capacity (LC %)

The encapsulation efficiency of each formulation was determined. Approximately 5 ml volume of each formulation was placed in a centri-

Table 1. Optimized formula for the preparation of the non-PEGylated and PEGylated NLCs.

Lipid matrix		5.0 % w/w
Metformin		1.0 % w/w
Polysorbate® 80 (Tween® 80)		2.0 % w/w
Sorbitol		4.0 % w/w
Water	q.s. to	100 % w/w

fuge tube and the tubes assembled in a centrifuge (TDL-4 B. Bran Scientific and Instru. Co. England) and centrifuged for 30 min at an optimized speed of 4000 rpm to obtain two phases (the aqueous and lipid phases). A 1 ml volume of the aqueous phase was measured out using a syringe and then diluted 10, 000 - fold using distilled water. The absorbance readings of the dilutions were obtained using a UV-VIS spectrophotometer (6405 Jenway, Dunmow, UK)) at a predetermined wavelength of maximum absorption of 231.5 nm. The amounts of drug encapsulated in the NLCs were calculated with reference to the standard Beer-Lambert's plot for metformin in distilled water, while the EE % was calculated using Eqs. (1) or (2):

$$Encapsulation\ efficiency\ (EE\ \%) = \frac{Actual\ drug\ content}{Theoritical\ drug\ content} \times 100 \quad \text{Eq. (1)}$$

$$EE\ \% = \frac{[Total\ drug - Drug\ in\ aqueous\ phase]}{[Total\ drug\ load]} \times 100 \quad \text{Eq. (2)}$$

LC is expressed as the ratio between the entrapped drug by the lipid and the total quantity of the lipids used in the formulation. This was calculated using Eq. (3):

$$Loading\ capacity = \frac{Total\ quantity\ of\ drug\ entrapped\ by\ the\ lipid}{Total\ quantity\ of\ the\ lipid\ in\ the\ formulation} \times 100 \quad \text{Eq. (3)}$$

2.4. In vitro drug release study

The USP XXII rotating paddle apparatus (Erweka, GmbH Germany) was employed for this release study using the dialysis technique [27]. The release medium consisted of 500mL of freshly prepared phosphate buffered saline (PBS, 0.1 M, pH = 7.4) maintained at 37 ± 1 °C by means of a thermostatic water bath. The polycarbonate dialysis membrane (length 7 cm, diameter 4 cm, MWCO 10,000; Spectrum, Los Angeles, USA) used as a release barrier was pre-treated by soaking in the release medium for 24 h prior to the commencement of each release experiment. In each case, 2 ml of the drug-loaded non-PEGylated and PEGylated NLCs, and one (500 mg) commercially available metformin hydrochloride tablet (Glucophage®) was placed in the dialysis membrane, securely tied with a thermo-resistant thread and then immersed in the release medium under agitation provided by the paddle at 100 rpm. At predetermined time intervals (30, 60, 120, 180, 240, 300, 360, 420, 480 and 600 min), 5 mL portions of the release medium were withdrawn and replaced with equal volume (5 mL) of the medium, thermostatically heated to the same temperature to maintain a sink condition), filtered with a pore size of 0.22 mm (Millipore filter, Delhi, India), and analyzed spectrophotometrically (6405 Jenway, Dunmow, UK)) at a wavelength of maximum absorption of 231.5 nm. The amount of drug released at each time interval was determined with reference to the standard Beer's plot for metformin in PBS. The percentage of metformin released was plotted against time.

2.5. In vivo studies

2.5.1. Ethical approval and experimental animals

All applicable international, national and/or institutional guidelines for the care and use of animals were followed. All experimental protocols were conducted with strict adherence to the guidelines of the Institutional Animal Care and Use Committee of the University of Nigeria, Nsukka. Ethical clearance approval for *in vivo* antidiabetic studies was sought and obtained from the Faculty of Pharmaceutical Sciences Research Ethics Committee (UNN/FPS/2019–2020_017X) before the commencement of the *in vivo* animal studies.

Wistar albino rats of both sexes weighing between 150 to 200 g were bred in the Faculty of Veterinary Medicine, University of Nigeria, Nsukka. The animals were housed in standard environmental conditions, kept at temperature of 37 ± 1 °C using warming lamps and left for one week to acclimatize with the new laboratory environment while being fed with standard laboratory low chow diet. All the animals were fasted for 12 h, but were allowed free access to water before the commencement of the antidiabetic studies.

2.5.2. Induction of experimental diabetes

Rats of either sex weighing 150–200 g were fasted for 12 h before the induction of diabetes, which was done by a single intraperitoneal injection of freshly prepared solution of alloxan monohydrate in normal saline (0.9 % NaCl) dosed at 150 mg/kg for all the groups. After 1 h of alloxan administration, the animals were fed freely and 5 % dextrose solution was also given orally in a feeding bottle for a day to overcome the early hypoglycemic phase. The animals were observed and found to have frequent urination, and after 48 h, blood was withdrawn from the tail vein of the animals and the blood glucose level measured with a glucometer (Accu-check, Roche, USA). The diabetic rats (glucose level above 200 mg/dl) were selected and separated to be used in the evaluation of antidiabetic activity and randomly divided into ten different groups (n = 6). Animal ethical procedures were strictly followed in accordance with the requirements of the Ethical Committee, Faculty of Pharmaceutical Sciences, University of Nigeria, Nsukka.

2.5.3. Evaluation of anti-diabetic activity

Sixty (60) diabetic (glucose level above 200 mg/dl) Wistar rats (either sex) were used for the evaluation of the anti-diabetic effects of the formulations. The diabetic rats were divided into ten groups of six animals in each group, and each group of animals was housed in a separate cage. The sample batches were administered orally to the animals as follows:

- Group I: received the test formulation (batch G_0) equivalent to 100 mg/kg dose of metformin hydrochloride.
- Group II: received the test formulation (batch G_{10}) equivalent to 100 mg/kg dose of metformin hydrochloride.
- Group III: received the test formulation (batch G_{20}) equivalent to 100 mg/kg dose of metformin hydrochloride.
- Group IV: received the test formulation (batch G_{40}) equivalent to 100 mg/kg dose of metformin hydrochloride.
- Group V: received the test formulation (batch G_{10}) equivalent to 50 mg/kg dose of metformin hydrochloride.
- Group VI: received the test formulation (batch G_{20}) equivalent to 50 mg/kg dose of metformin hydrochloride.
- Group VII: received the test formulation (batch G_{40}) equivalent to 50 mg/kg dose of metformin hydrochloride.
- Group VIII: received Glucophage® equivalent to 100 mg/kg dose of metformin hydrochloride (first positive control).
- Group IX: received pure metformin equivalent to 100 mg/kg dose of metformin hydrochloride (second positive control).
- Group X: received normal saline per orally (negative control).

All the samples for treatment were administered orally. Blood samples of the animals were collected from the tail vein afterwards at time intervals of 0, 1, 3, 6, 12, and 24 h and tested for blood glucose level using the glucometer. The post-dose levels of the blood glucose were expressed as a percentage of the pre-dose level using Eq. (4).

$$\%\ \text{Glycaemic change} = \frac{\text{Initial Conc} - \text{Final Conc}}{\text{Initial Conc}} \times 100 \quad \text{Eq. (4)}$$

2.5.4. Oral bioavailability study

Eighteen (18) rats were made diabetics as described in the preceding section on antidiabetic study, randomly divided into three groups of six rats each and orally administered with the formulations as follows:

Group I: received the MT-loaded non-PEGylated NLC formulation (batch G_0) equivalent to 100 mg/kg dose of metformin hydrochloride.

Group II: received the MT-loaded PEGylated NLC formulation (batch G_{20}) equivalent to 100 mg/kg dose of metformin hydrochloride.
Group III: received Glucophage® (reference sample) equivalent to 100 mg/kg dose of metformin hydrochloride (positive control).

Blood samples of the animals were collected from the tail vein afterwards at time intervals of 0, 1, 3, 6, 12, and 24 h using heparinized hematocrit tubes. The heparinized blood samples were centrifuged at 5,000 rpm for 5 min to separate the plasma, which were stored at -4 °C till analyzed. For each sample, 0.2 ml of the plasma sample was deproteinated by diluting with equal volume of acetonitrile and centrifuged at 2,000 rpm for 5 min. Then 0.1 ml of the supernatant was diluted in distilled water and assayed for drug content using a digital spectrophotometrically (Unico 2102 PC UV/Vis Spectrophotometer, New York, USA). The plasma from the blood withdrawn at zero hour was similarly diluted and used as blank and for the preparation of calibration curve. Amounts of drug in the plasma were plotted against time to obtain the plasma concentration time curve, which was further evaluated to obtain the pharmacokinetic parameters including the maximum plasma concentration (C_{max}) and the corresponding time (T_{max}) which were determined directly from the concentration-time data.

2.6. Statistical analysis

All experiments were performed in replicates for validity of statistical analysis. Results were expressed as mean ± SD. ANOVA and Student's t-test were performed on the data sets generated using SPSS. Differences were considered significant for p-values < 0.05. The pharmacokinetic parameters were calculated using Phoenix® WinNonlin (version 6.3; Pharsight, St Louis, MO, USA), based on the average blood drug concentration. Area under the curve (AUC) from 0 to 24 h was calculated using the program's linear trapezoidal rule. Maximum plasma concentration (C_{max}) and time needed to reach the maximum plasma concentration (T_{max}) were determined directly from the concentration-time data.

3. Results and discussion

3.1. Thermal characterization

The thermal properties of beeswax, Phospholipon® 90H, the plain lipid matrices (LM_1 and LM_3), PEG – 4000, the PEGylated lipid matrix 3 (PEG - LM_3), metformin, the drug-loaded lipid matrix (i.e. LM_3) and the drug - loaded PEGylated lipid matrix (i.e. PEG – LM_3) are shown in Table 2 while their respective DSC thermographs are depicted in Figures 1a-f and 2. Differential scanning calorimetry (DSC) is commonly used to measure the heat loss or gain resulting from physical or chemical changes within a sample as a function of temperature. This provides a means through which the state, melting/thermal and crystallization properties of lipid nanoparticles, including NLCs, can be studied and characterized. The mixing pattern/behaviors of the component solid and liquid lipids of NLC, as well as those of other components of the formulation can be investigated using DSC [8, 18, 28]. The melting endotherm of LM_1 (mixture of solid lipids i.e. beeswax, BW and Phospholipon® 90H, P90H) was observed to be 88.6 °C with an enthalpy of – 32.5 mW/mg while that of LM_3 was observed to be 107.5 °C with an enthalpy of – 4.5 mW/mg Figure 1c and 1d show that with LM_1 (solid lipids only), the peak was a steep slope – a sharp endothermic peak - (in Figure 1c) while with LM_3 (having the liquid lipid – Capryol PGE 860 – in the lipid blend), the peak gradually broadened (showing an increase in the width of melting area, mostly from the onset point to the end of the melting process) – (in Figure 1d). This increase/broadening indicates more imperfection in the crystal structure and normally pronounced in lipid-based drug delivery systems such as NLCs with higher content of the liquid lipid [8, 28]. The DSC profile of PEG – 4000 showed a sharp endothermic peak corresponding to a slightly low melting peak of 74.5 °C. However, when the lipid matrix (LM_3) was PEGylated, the PEG reduced the melting point of the resulting combination to 90.5 °C with an enthalpy of – 14.2 mW/mg. This melting point depression is normally observed when one compound dissolves in another compound, and indicates good miscibility of the components and can be attributed to the ability of the PEG to reduce the crystallinity of the lipids [28]. The melting endothermic peak of metformin was obtained as 265.5 °C with an enthalpy of - 28.4 mW/mg (Figure 2a). The drug – loaded LM_3 was observed to have a melting endothermic peak of 93.5 °C (Figure 2b) indicating that the non-PEGylated lipid was able to reduce the crystallinity of the drug while that for the drug–loaded PEG–LM_3 was observed to be 85.6 °C with an enthalpy of – 3.2 mW/mg (Figure 2c), indicating that the PEGylated lipid was able to further reduce the crystallinity of the drug (than the non-PEGylated lipid). The probable distortion of the crystal structure of the lipids leading to the observed reduction in the endothermic peaks may be of advantage in drug encapsulation. The DSC thermograms of the metformin–loaded non-PEGylated and PEGylated lipid matrices showing no drug melting peak between the ranges of 100 °C–200 °C indicate that the drug was not in crystalline form but rather in the amorphous form. These observances are similar to the findings on NLCs reported in the literature [8, 18]. The amorphous form would have higher energy with increased surface area, subsequently higher solubility, dissolution rates and bioavailability, consistent with earlier report [8].

Table 2. Thermal properties of PEG-4000, drug, plain and drug-loaded non-PEGylated and non-PEGylated lipid matrices.

Sample	Melting peak (°C)	Enthalpy (mW/mg)	Type of peak
Beeswax	73	-55.3	Endothermic
Phospholipon® 90H (P90H)	122.1	-38.9	Endothermic
	88.6	-32.5	Endothermic
LM_1	107.5	-4.5	Endothermic
LM_3	278.3	2.1	Exothermic
PEG-4000	74.5	-3.8	Endothermic
PEG-LM_3	90.5	-14.2	Endothermic
Metformin	265.5	-28.4	Endothermic
Drug-loaded LM_3	93.5	-4.0	Endothermic
	257.0	-7.6	Endothermic
Drug-loaded PEG-LM_2	85.6	-3.2	Endothermic
	93.5	-2.1	Endothermic
	256.0	-4.9	Endothermic

3.2. Fourier transform infra-red (FT-IR) spectroscopy of drug and drug-loaded lipid matrices

The results for the FT-IR spectroscopic analysis of metformin (MT), MT – loaded LM_3, and MT – loaded PEG – LM_3 are presented in Table 3 as well as in Figure 3. Significant changes in the characteristic bands of the FT-IR spectra were observed, suggesting an alteration in drug micromilieu. The diagnostic absorption peaks and the type of bonds of MT, when compared to that of MT-loaded LM_3, showed that the absorption bands at 1219.05 cm^{-1} (C–O vibration) and 601.81 cm^{-1} (C–H out of plane bending) obtained with MT is absent with MT-loaded LM_3. This suggests an interaction between the two components, which might facilitate the effective solubilization and incorporation of MT into the lipid materials. Interestingly, the PEGylation of LM_3 resulted in the restoration of the absorption band at 1219.05 cm^{-1} (C–O vibration), and may be ascribable to the formation of non-covalent bonds (e.g., hydrogen bond, hydrophilic interaction) between the groups containing an electronegative nitrogen (N) atom of MT and the ether oxygen group of PEG, and the generation of the absorption band 964.44 cm^{-1} (N–H out of plane bending). Also the diagnostic absorption peaks and the type of bonds of MT-loaded LM_3, when compared to that of MT-loaded PEG-LM_3, showed that the absorption bands at 2345.52 cm^{-1} (-C=C- stretching)

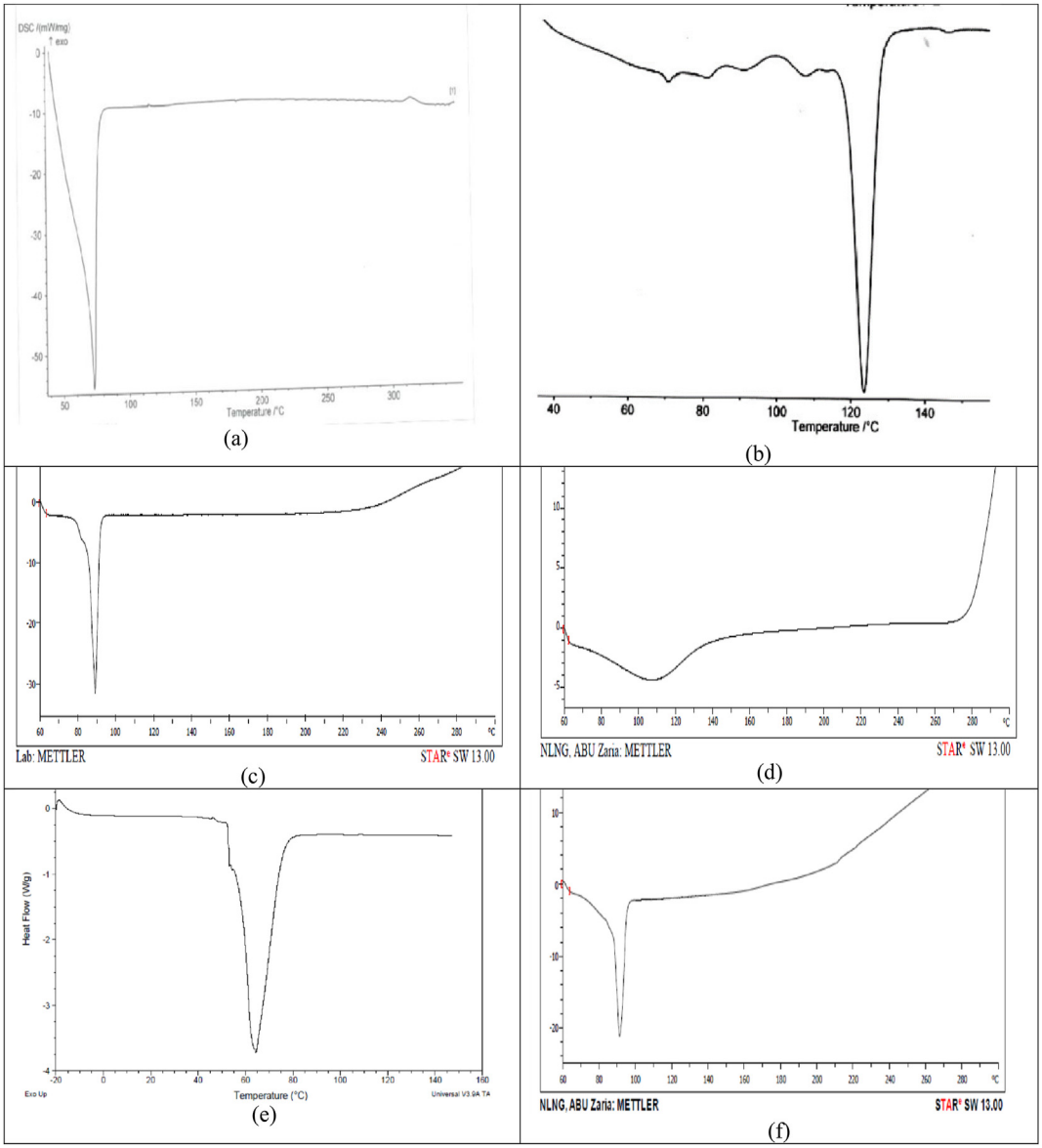

Figure 1. Differential scanning calorimetry (DSC) thermograph of (a) beeswax (BW), (b) Phospholipon® 90H (P90H), (c) structured lipid matrix (BW:P90H) (7:3) (LM_1), (d) Phospholipid-modified beeswax-based lipid matrix structured with capryol-PGE 860 (LM_3), (e) PEG 4000, and (f) PEGylated lipid matrix (PEG-LM_3).

obtained with the former is absent in the later. This also suggests an interaction between PEG and the lipid matrix which might facilitate the conjugation of PEG onto the lipid matrix through the formation of a covalent bond (e.g., lipophilic interaction). Hence, other major peaks present in MT and in the MT-loaded LM_3, except for those mentioned above, were also observed in the combinations, indicating areas of no significant chemical interaction. Also, no peaks indicating incompatibilities resulting from the formation of an entirely different/new entity were observed in the FT-IR spectrums; thus, indicating compatibility between the drug and excipients used in the formulations.

3.3. Mean particle sizes, polydispersity indices and surface charges of the developed formulations

The photon correlation spectroscopy (PCS) analysis results (particle size distribution by intensity) of the capryol-based non-PEGylated and PEGylated nanostructured lipid carriers are depicted in Figure 4 whereas Figure 5 shows the diagrammatic representation of the mean particle sizes and the polydispersity indices (PDIs) of the various batches of the NLC formulations (non-PEGylated and PEGylated). The mean particle sizes for non-PEGylated NLC (G_0), PEGylated NLC (G_{10}), PEGylated NLC (G_{20}), and PEGylated NLC (G_{40}) containing 0, 10, 20 and 40% of PEG-4000, respectively, in the lipid matrix used in the nanoparticles formulation, were observed as 305.90, 184.80, 268.40, and 882.50 nm, respectively while their PDIs were 0.368, 0.548, 0.58, and 0.687, respectively. Particle characterization is essential to ensure the production of stable colloidal systems of suitable quality [29]. Meanwhile, all the particles were within the nanometer ranges as expected of a well formulated NLC. Batch PEG – NLC (G_{10}) had the narrowest particle size, and as such would be expected to provide a better stability with little or no chance for particle growth. Also, it was observed that the 10 % PEGylated NLC (G_{10}) has reduced mean particle size compared to the non-PEGylated NLC (G_0). This decrease could be attributed to the properties and actions of PEG on the NLC, and agrees with findings by other researchers [29, 30, 31, 32]. PEG, being a non-ionic surfactant has been reported to effect reduction in particulate sizes when intercalated onto lipid layers. This effect is associated with the formation of resistant closely packed mixed films on interaction with lipid layer. These results are consistent with those of previous findings [29, 30, 31, 32]. The result also showed that increasing the

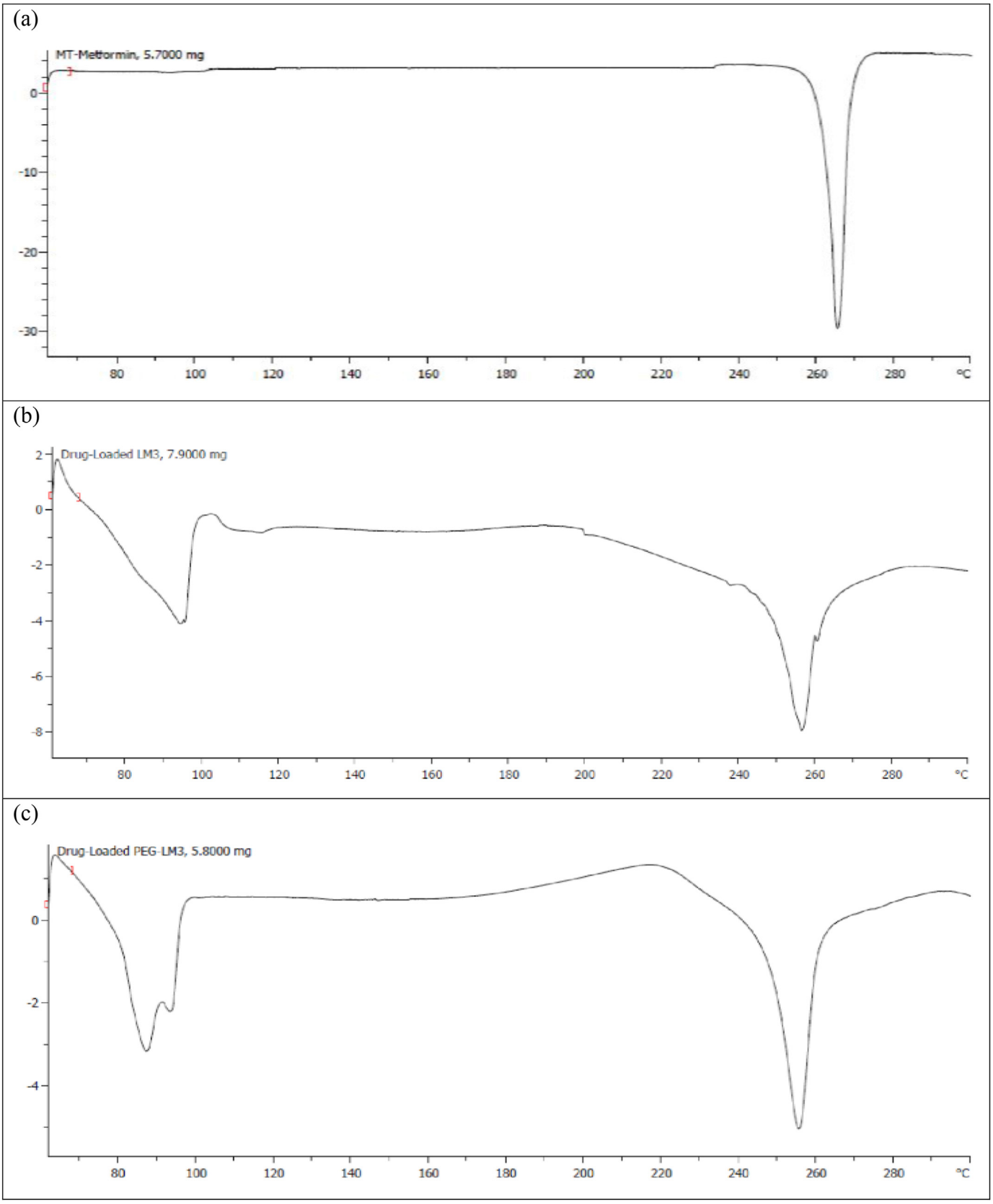

Figure 2. DSC thermographs of sole MT (a) and MT-loaded non-PEGylated (b) and PEGylated lipid matrices (c).

Table 3. Fourier transform infra-red (FT-IR) profiles of MT, MT-loaded PEGylated and MT-loaded non-PEGylated lipid matrices.

Sample	Principal peak (cm^{-1})	Type of bond
Metformin (MT)	3456.55	N–H stretching
	2931.90	$(CH_3)_2$–N absorption
	1643.41	N–H deformation
	1396.51	N–H deformation
	1219.05	C–O vibration
	1103.32	C–N stretching
	1130.74	C–N stretching
	771.56	N–H wagging
	601.81	C–H out of plane bending
	547.8	C–N–C deformation
MT-loaded LM_3	3379.40	N–H stretching
	2916.47	$(CH_3)_2$–N absorption
	2345.52	-C=C- stretching
	1728.28	Conjugated C=C bond vibration
	1651.12	N–H deformation
	1573.97	N–H deformation
	1458.23	N–H deformation
	1396.51	N–H deformation
	1195.91	C–N stretching
	1072.46	C–N stretching
	856.42	NH_2 rocking
	748.41	N–H wagging
	717.54	N–H wagging
	532.37	C–N–C deformation
MT-loaded PEG-LM_3	3387.11	N–H stretching
	2916.47	$(CH_3)_2$–N absorption
	2854.74	$(CH_3)_2$–N absorption
	1728.28	Conjugated C=C bond vibration
	1651.12	N–H deformation
	1581.68	N–H deformation
	1458.23	N–H deformation
	1396.51	N–H deformation
	1219.05	C–O vibration
	1103.32	C–N stretching
	964.44	N–H out of plane bending
	848.71	NH_2 rocking
	771.55	N–H wagging
	717.54	N–H wagging
	594.10	C–N–C deformation

percentage of PEG-4000 in the formulation from 10 % (G_{10}) to 20 % (G_{20}) and then to 40 % (G_{40}) increased the mean particle sizes from 184.80 to 268.40 and then to 882.50 nm respectively. These increments due to increasing percentages of PEG in the formulations are thought to adversely/negatively affect the overall particle behaviors while lower percentages of PEG show significant improvements in the overall particle behaviors as supported by previous findings in the literature [32]. Generally, PDI is a measure of the distribution of molecular mass in a given colloidal formulation [5]. The PDI values were all below 0.7, and values $\leq$0.7 is the range over the distribution algorithms best operates and implies that the NLC formulations are monodispersed particulate systems [33].

Furthermore, the formulations had zeta potentials or surface charges (>25 mV) as shown in Table 4, indicating good stability of the MT-loaded PEGylated and MT-loaded non-PEGylated NLC formulations. The positive surface charges on the formulations are very important in that they would aid in easily transporting the PEGylated and non-PEGylated NLC across cell membranes. More so, they can interact with negatively charged mucosa walls of the GIT to improve the binding of the positively charged particles to the GIT wall, and thus prolong drug release for enhanced absorption, consistent with previous reports [2, 15].

3.4. Scanning electron microscopy (SEM) of capryol-based drug-loaded non-PEGylated and PEGylated nanostructured lipid carriers

The scanning electron micrograph of a representative formulation of metformin-loaded capryol-based PEGylated NLC as depicted in Figure 6, showed that the drug-loaded PEGylated NLC nanoparticles were non-smooth, non-spherical and irregularly shaped, but with homogenous shading and almost several particle sizes spread all over the formulation corresponding to the broader particle size distribution observed in Figures 4 and 5 above as well as from the PDI values. Also, an interesting observation was the presence of well-defined nano-dispersions in the formulation. This is thought to be due to the formation of hydration shells on the surfaces of the nanostructures where water molecules associate with the hydrophilic PEG chains; thus preventing interaction, fusing and/or aggregation of the nanocarriers through steric hindrances [34].

3.5. Fourier transform infra-red spectroscopy of drug-loaded NLC formulations

The results of the FT-IR spectroscopic analysis of metformin, G_0 (drug-loaded non-PEGylated NLC), G_{10} (drug-loaded 10 % PEGylated NLC), G_{20} (drug-loaded 20 % PEGylated NLC), and G_{40} (drug-loaded 40 % PEGylated NLC) are presented in Table 5 as well as in Figure 7. The FT-IR spectrum of G_0, when compared to that of metformin, reveals the disappearance of the characteristic absorption bands at 771.56 cm^{-1} (N–H wagging) and 601.81 cm^{-1} (C–H out of the plane bending) found in metformin, indicating significant interaction between the drug and the lipid matrix which is probably needful for the solubilization and incorporation of the drug into the lipid matrix. The FT-IR spectrum of G_{10}, when compared to that of metformin, reveals the disappearance of the characteristic absorption band at 1219.05 cm^{-1} (C–O vibration) indicating interaction between metformin and PEG by hydrophilic bonding/interaction, such as hydrogen bonding, through the hydrophilic groups of PEG, and resulting in the formation of a new characteristic absorption band at 2353.23 cm^{-1} (-C=C- stretching). This interaction is thought to further enhance the solubilization of metformin in the formulation. The FT-IR spectra of G_{20} and G_{40} were almost identical with no significant differences indicating that increasing the PEG concentration/density in the formulation did not culminate into any significant interaction, and instead resulted in the restoration of the C–O vibration formerly found in metformin but at a different characteristic absorption band of 1257.63 cm^{-1}. Hence, other major peaks present in metformin and in the G_0, except for those mentioned above, were also observed in the combinations with PEG, indicating areas of no significant chemical interaction. Also, no peaks indicating incompatibilities resulting from the formation of an entirely different/new entity were observed in the FT-IR spectra.

3.6. Encapsulation efficiency (EE) and loading capacity (LC) of PEGylated and non-PEGylated NLCs

The results obtained from the determination of the encapsulation efficiencies and loading capacities of the non-PEGylated (G_0) and 10, 20, and 40 % PEGylated (G_{10}, G_{20}, and G_{40} respectively) capryol-based NLC formulations are shown in Figure 8. The EE for G_0, G_{10}, G_{20} and G_{40} were 99.12, 98.95, 99.65, 98.61 % respectively while their loading capacity were 16.54, 16.52, 16.62, and 16.47 per 100 mg, respectively. Encapsulation efficiency gives succinct information regarding the percentage amount of drug entrapped/encapsulated by the nanoparticles while the loading capacity provides information on the amount of the drug (in mg) that each 100 mg of the nanoparticle contains. It was

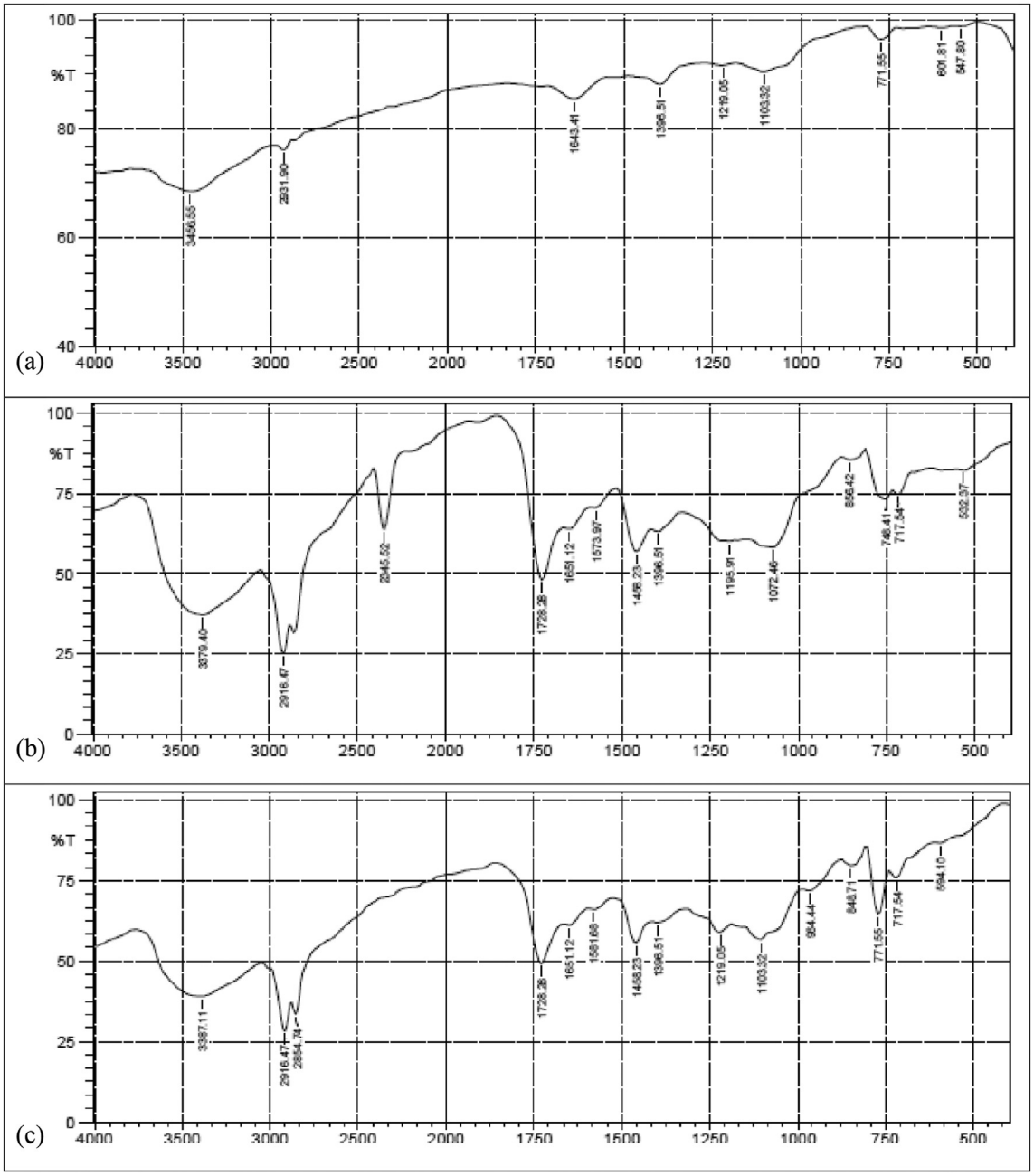

Figure 3. FT-IR spectra of sole MT (a) and MT-loaded non-PEGylated (b) and PEGylated lipid matrices (c).

reported that a second type of NLCs is formed when the lipid molecules used, as in this case, are chemically very different, resulting in a structure with many internal imperfections; thus, making available sufficient spaces to accommodate the drug [8], culminating into high entrapment/encapsulation efficiency and loading capacity. Approximately, the results show that PEGylation slightly increases the encapsulation efficiency of the formulation. On the other hand, comparing the effect of the different percentages of PEG in the formulation renders 20 % PEGylation an optimized level of PEGylation for enhanced drug loading and encapsulation. Metformin, loaded into the nanocarriers, is a hydrophilic molecule; this means that the NLC formulations increased the solubility of the drug as they enhance encapsulation of the metformin, with PEGylation being a mild enhancement factor. This is an advantage for our work.

3.7. In vitro drug release from the metformin-loaded PEGylated and non-PEGylated NLCs

Figure 9 shows the *in vitro* drug release profile of metformin-loaded non-PEGylated (G_0) and PEGylated (G_{10}, G_{20} and G_{40}) capryol-based nanostructured lipid carriers. From the figure, it could be seen that the formulations (both non-PEGylated and PEGylated NLCs) had sustained and higher cumulative drug released (%) than the commercial metformin formulation (Glucophage®). Also, it was observed that the 10 % PEGylated (G_{10}) and 40 % PEGylated (G_{40}) NLCs had the highest cumulative drug released (%) after 10 h, followed by 20 % PEGylated (G_{20}) and non-PEGylated NLCs having almost equivalent release, while the commercial metformin sample (Glucophage®) had the least cumulative drug release (%) with an initial burst release of metformin and retarding release when

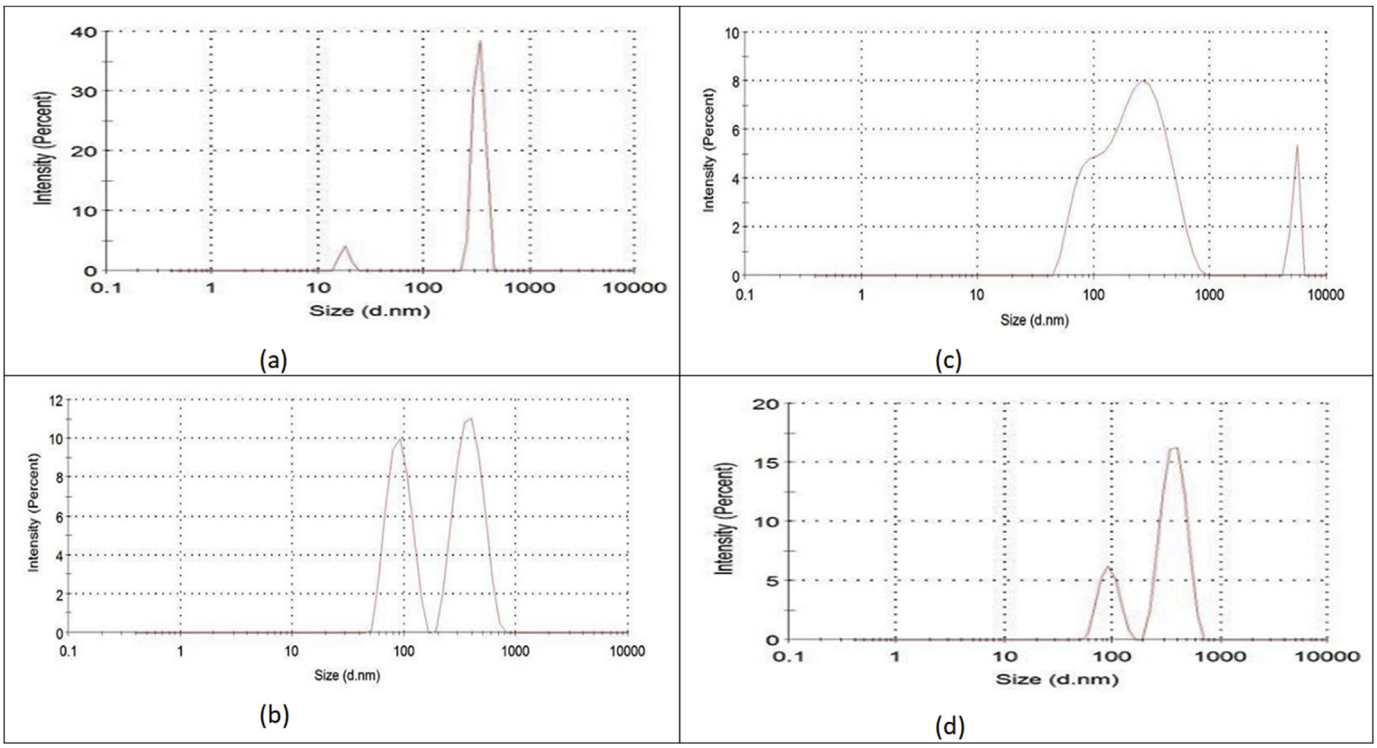

Figure 4. Particle size distribution by intensity of metformin-loaded capryol-based non-PEGylated nanostructured lipid carrier (batch G_0) (a), PEGylated nanostructured lipid carrier (batch G_{10}) (b), PEGylated nanostructured lipid carrier (batch G_{20}) (c) and PEGylated nanostructured lipid carrier (batch G_{40}) (d).

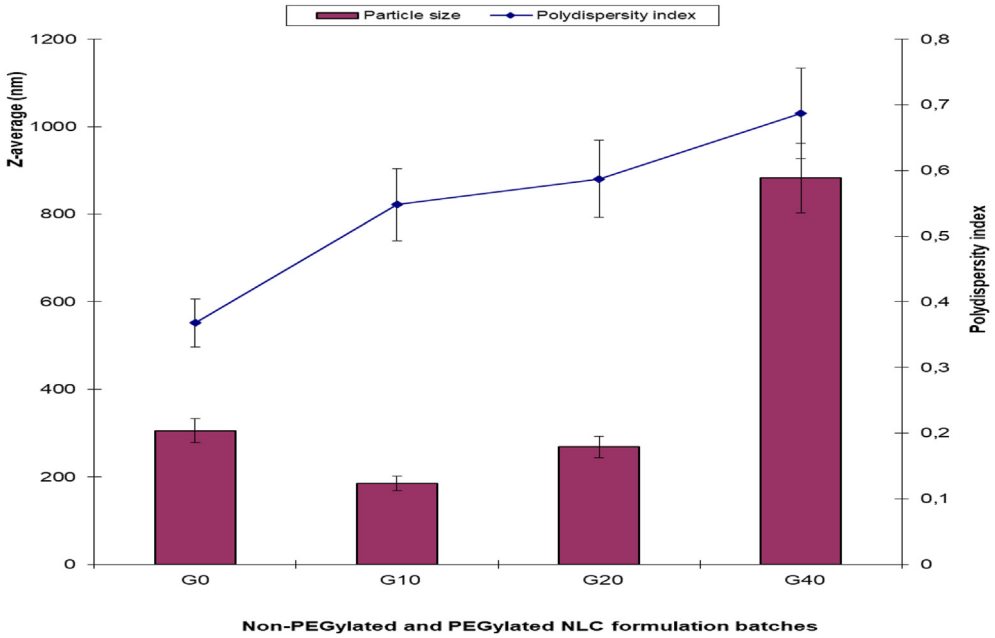

Figure 5. Mean particle sizes and polydispersity indices of the metformin-loaded capryol-based non-PEGylated and PEGylated nanostructured lipid carriers.

Table 4. Surface charges of MT-loaded PEGylated and MT-loaded non-PEGylated nanostructured lipid carriers.

Samples	Zeta potential/Surface charge (mV)
G_0	26.5 ± 0.61
G_{10}	30.0 ± 0.47
G_{20}	28.6 ± 0.20
G_{40}	26.5 ± 0.01

respective release times are considered. This shows that PEGylation has the ability to improve the release of metformin from NLCs, consistent with earlier reports [10, 11].

3.8. Antidiabetic activity of the metformin-loaded PEGylated and non-PEGylated NLCs

Figure 10 shows the result of the anti-hyperglycemic activities produced by 50 and 100 mg/kg doses of both non-PEGylated (G_0) and

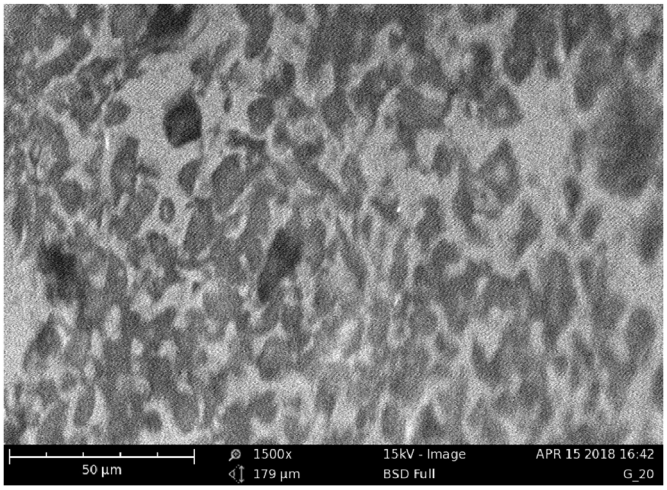

Figure 6. Scanning electron micrograph (SEM) of metformin-loaded capryol-based PEGylated nanostructured lipid carrier (batch G_{20}) (representative formulation).

PEGylated (G_{10}, G_{20}, and G_{40}) capryol-based metformin-loaded NLCs in comparison with those produced by 100 mg/kg of both commercial metformin sample (Glucophage®) and pure metformin sample (positive controls), and distilled water (negative control) in alloxan-induced diabetic rats. The result shows that G_0, G_{20}, G_{40} at 100 mg/kg and G_{10} and G_{20} at 50 mg/kg produced higher % reduction in blood glucose level than the positive control (commercial metformin sample - Glucophage®) over a period of 24 h. This suggests that the formulations, even at reduced doses, were effective in the treatment of diabetes. This proves the ability of the formulations to enhance the bioavailability of the drug –metformin - incorporated into the nano-carriers. This would culminate in the possibility of reducing the high dosing of metformin, as seen with Glucophage®, in the treatment of diabetes, thereby reducing the side effects/dose-related adverse effects associated with metformin, leading to reduction in dosing frequency and enhancing patients' compliance to the administration of metformin as an oral anti-hyperglycemic agent. Notwithstanding, the result also shows that G_{10} dosed at 100 mg/kg and G_{40} dosed at 50 mg/kg did not yield any better antidiabetic activities than Glucophage®. A possible explanation to the inefficacy of G_{10} dosed at 100 mg/kg is poor experimental procedure as regards to its administration during the animal studies or the possibility of administering incorrect dose to the experimental animals, because a lower dose of the same formulation (50 mg/kg of G_{10}) proved to be effective in exerting its antidiabetic effects over the 24 h period. On the other hand, possible explanations to the inefficacy of G_{40} include the reduced dose (50 mg/kg), coupled with the effect of PEG density on the formulation. The literature has pointed out the characteristics of the bond between PEG and small molecules, such as nanoparticles, reveals that modifications with PEG could either result in "permanent" or "releasable" PEGylation [35].

Permanent PEG links create novel compounds for increasing oral bioavailability and decreasing penetration of specific barriers and generally requires low molecular-weight PEGs (Mw $<$ 1000 Da) because macromolecular PEGs may block activity of small active agents at the target cells via steric hindrance [35]. G_{40} containing 40 % of PEG 4000 of molecular weight 3500–4500 g/mol and bulk density of 400–500 kg/m^3 could be considered macromolecular or to have higher surface density than 10 and 20 %. PEG density was calculated based upon the concentration of particles in solution and the surface area of hydrated particles [32]. Comparing the anti-hyperglycemic activities of the non-PEGylated and PEGylated metformin loaded NLC, reveals that the non-PEGylated produced a higher but time-dependent decrease in activity while the effective PEGylated NLCs showed sustained increasing anti-hyperglycemic activity with time. The possible explanation for this is that G_0 had higher encapsulation efficiency, and non-PEGylated nanoparticles, when administered, have higher tendencies to be bound by serum albumins and easily cleared from the blood through associations with macrophage phagocytic system (MPS) than PEGylated nanoparticles [32, 36]. The effects of PEGylation are highly dependent on the PEG molecular weight (MW), polymer chain architecture, and surface density of the PEG coating, which leads to transitions in PEG conformations (mushroom conformation – for low density PEGs or brush conformation – for high density PEGs) at the surface. PEGylations using large molecular-weight PEGs (1000–60,000 Da) have been found to enhance water solubility, modify biodistribution, and increase the circulating half-lives of nano-particulate drug formulations by significantly reducing protein adsorption and macrophage association,

Table 5. Fourier transform infra-red (FT-IR) profiles of MT and MT-loaded capryol-based PEGylated and non-PEGylated nanostructured lipid carriers.

Sample	Principal peak (cm^{-1})	Type of bond
Metformin	3456.55	N–H stretching
	2931.90	$(CH_3)_2$–N absorption
	1643.41	N–H deformation
	1396.51	N–H deformation
	1219.05	C–O vibration
	1103.32	C–N stretching
	1130.74	C–N stretching
	771.56	N–H wagging
	601.81	C–H out of plane bending
	547.8	C–N–C deformation
G_0	3927.20	N–H stretching
	3772.89	N–H stretching
	3371.68	N–H stretching
	2808.45	$(CH_3)_2$–N absorption
	2152.63	Carboxylic acid C=O vibration
	1643.41	N–H deformation
	1234.48	C–O vibration
	1080.17	C–N stretching
	563.23	C–N–C deformation
G_{10}	3796.04	N–H stretching
	3325.39	N–H stretching
	2931.90	$(CH_3)_2$–N absorption
	2569.27	$(CH_3)_2$–N absorption
	2353.23	-C=C- stretching
	2006.04	Carboxylic acid C=O vibration
	1411.94	N–H deformation
	1026.16	C–N stretching
	478.36	C–N–C deformation
G_{20}	3363.97	N–H stretching
	2931.90	$(CH_3)_2$–N absorption
	2106.34	Carboxylic acid C=O vibration
	1643.41	N–H deformation
	1473.66	Symmetric N–H deformation
	1249.91	C–O vibration
	1080.17	C–N stretching
	547.80, 455.22	C–N–C deformation
G_{40}	3371.68	N–H stretching
	2885.60	$(CH_3)_2$–N absorption
	2800.73	$(CH_3)_2$–N absorption
	2044.61	Carboxylic acid C=O vibration
	1643.41, 1388.79	N–H deformation
	1257.63	C–O vibration
	1080.17	C–N stretching
	540.09	C–N–C deformation

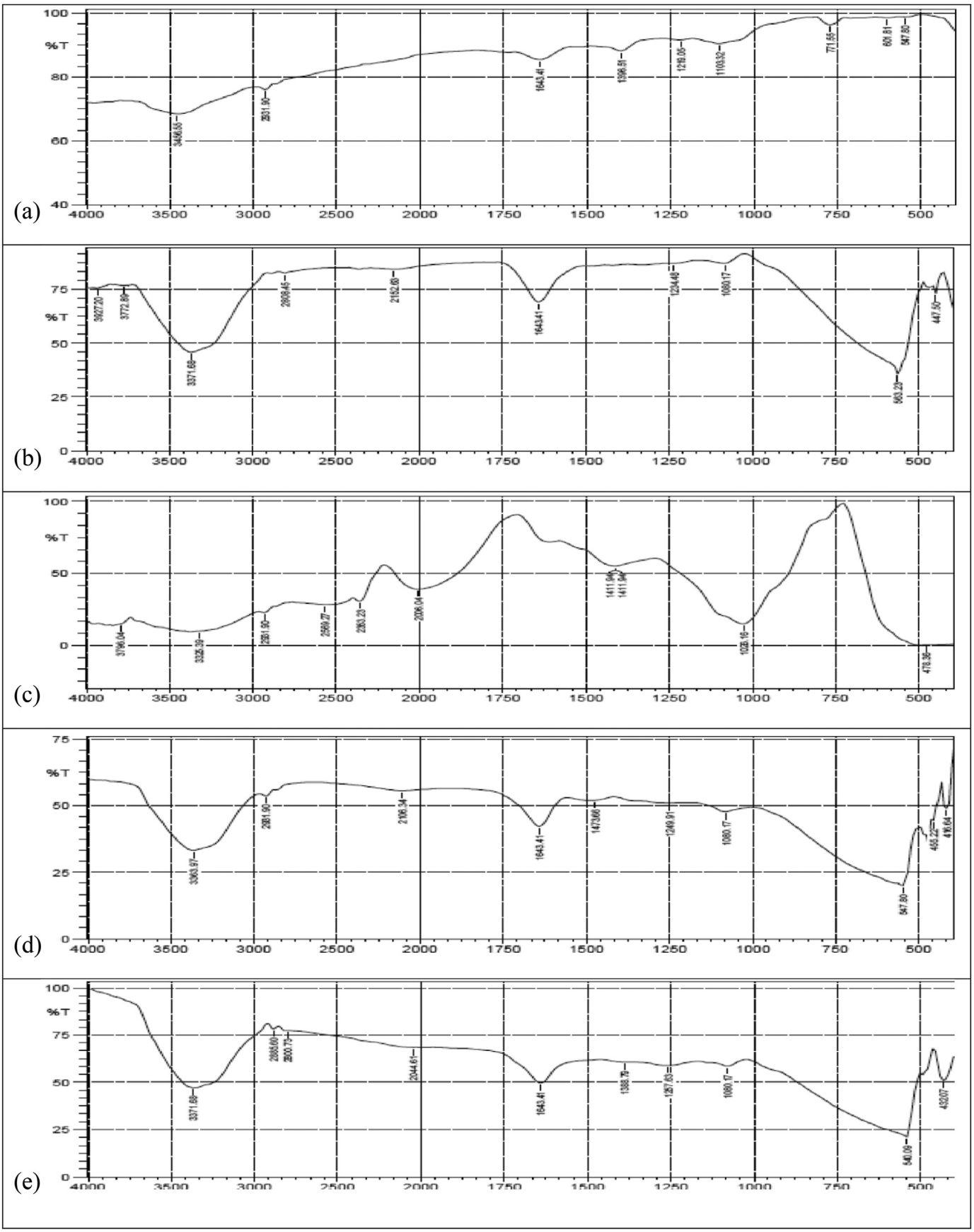

Figure 7. FT-IR spectra of Metformin (a) and metformin-loaded non-PEGylated and PEGylated capryol-based nanostructured lipid carriers (G_0, G_{10}, G_{20} and G_{40}) (b–e) in superposition.

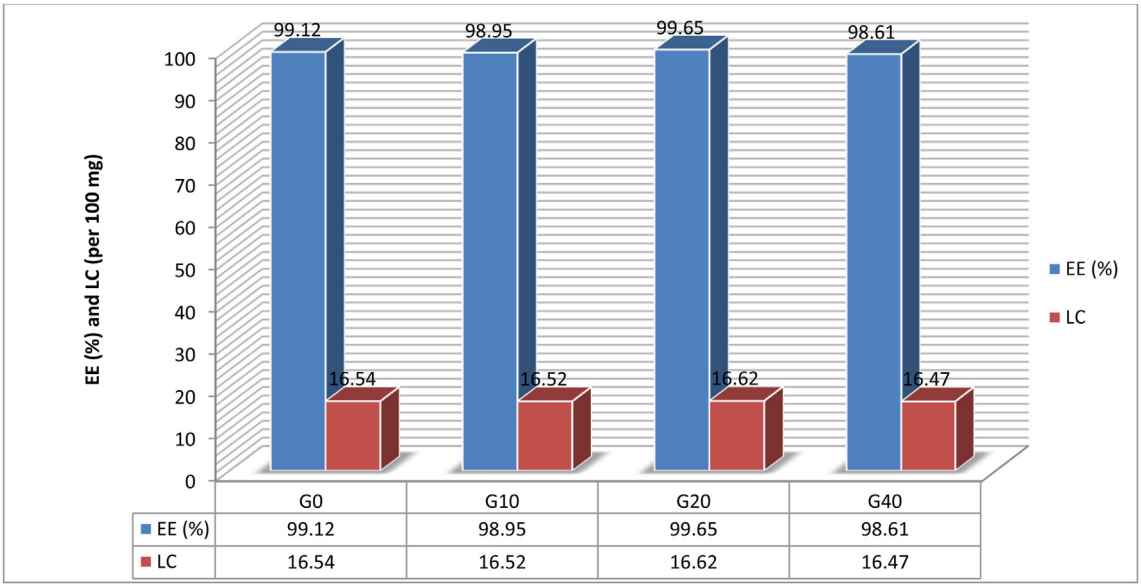

Figure 8. Diagrammatic representations of the encapsulation efficiency and loading capacity of the metformin-loaded PEGylated and non-PEGylated NLC formulation.

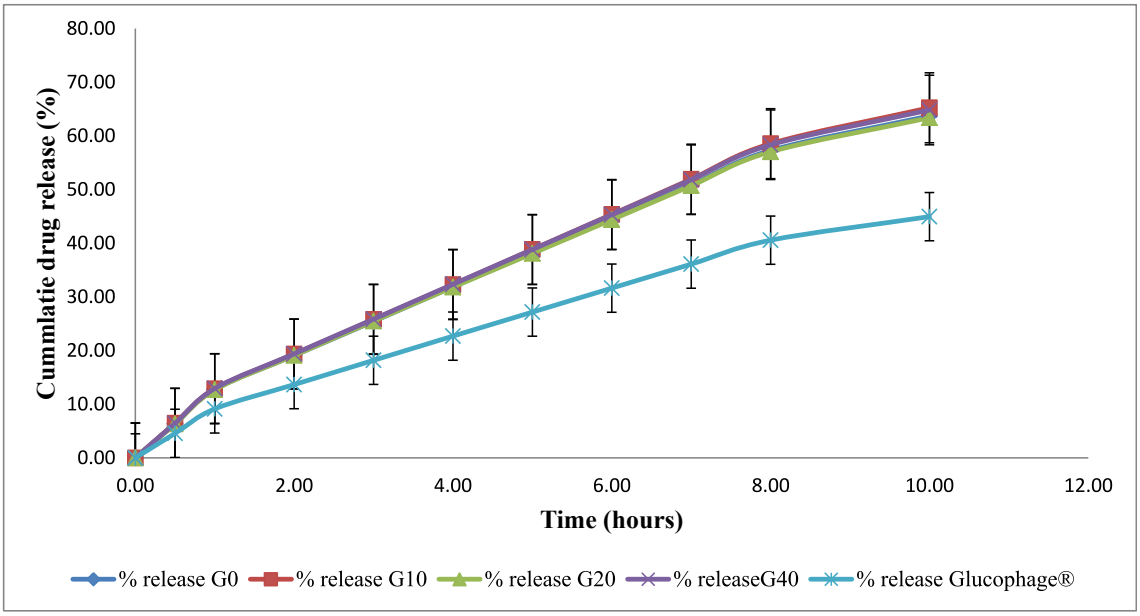

Figure 9. *In vitro* release pattern of drug-loaded non-PEGylated and PEGylated capryol-based NLC formulations in PBS (pH 7.4).

mucin binding, digestive enzyme actions, and metabolism. Significant improvement in overall particle behavior with lower PEG densities has also been reported [32, 36, 37, 38]. Furthermore, PEGylation has been reported to result in at least a 17-fold increase in circulation half-life, a 136-fold decrease in clearance, and an 86-fold increase in AUC over non-PEGylated NPs [32]. These provide the explanations to the sustained increasing anti-hyperglycemic activity with time seen with the effective metformin-loaded capryol-based formulations, even at reduced doses of 50 mg/kg.

3.9. Oral bioavailability of the metformin-loaded PEGylated and non-PEGylated NLCs

The plasma concentration–time profiles of metformin-loaded non-PEGylated and PEGylated NLC formulations are shown in Figure 11 whereas data obtained from the pharmacokinetic studies are shown in Table 6. The peak plasma level noted in the reference drug was attained rapidly and there was a quick fall in the plasma level within few hours of the study. When this was compared to the metformin-loaded non-PEGylated NLC and MT-loaded PEGylated NLC, although there was a delay in attaining the plasma peak, and the plasma concentrations were maintained for a longer period of time than the reference sample. More so, the mean plasma concentrations after an oral administration of the developed PEGylated and non-PEGylated NLC formulations of MT increased at broader peaks than the plasma concentrations of the marketed metformin formulation (Glucophage®, reference sample). The mean AUC_{-24} values for optimized metformin-loaded non-PEGylated and PEGylated NLC indicate approximately 3-fold and 5-fold increase in systemic bioavailability of metformin from metformin-loaded non-PEGylated and PEGylated NLC, respectively. Similarly, the mean C_{max} values for non-PEGylated and PEGylated NLC formulations were significantly ($p < 0.005$) greater than that for the reference because, while the

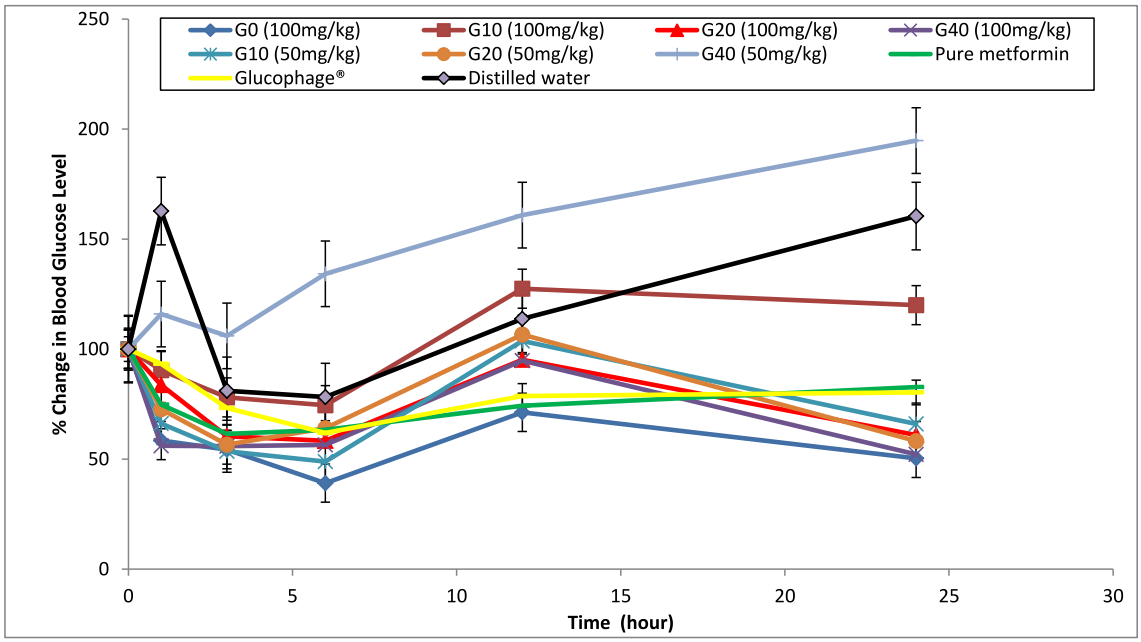

Figure 10. Percentage blood glucose reductions produced by 50 and 100 mg/kg doses of both non-PEGylated (G_0) and PEGylated (G_{10}, G_{20}, and G_{40}) capryol-based metformin-loaded NLCs, 100 mg/kg of both commercial metformin sample (Glucophage®) and pure metformin sample (positive controls), and distilled water (negative control) in alloxan-induced diabetic rats after predetermined time intervals.

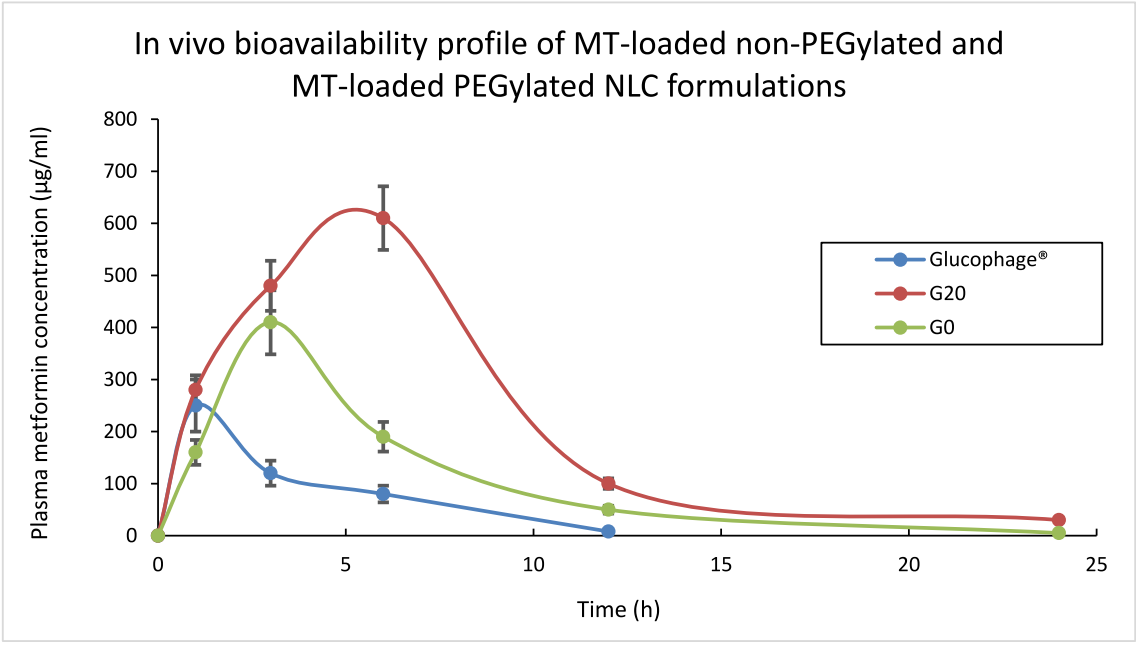

Figure 11. Changes of metformin concentration in blood over 24-h study period, of rats orally administered with the optimized MT-loaded PEGylated NLC (G_{20}) and MT-loaded non-PEGylated NLC (G_0) in comparison with marketed formulation (Glucophage®) at equivalent dose.

Table 6. Pharmacokinetic parameters of the MT-loaded non-PEGylated and PEGylated NLC formulations after oral administration to rats (mean ± SD, n = 6).

Sample	AUC (µg/mL.h)	C_{max} (µg/mL)	T_{max} (h)
G_0	1058.16 ± 3.04	398.69 ± 2.53	3.0
G_{20}	1850.98 ± 4.31	601.87 ± 1.92	5.5
Glucophage®	354.72 ± 2.06	249.48 ± 1.08	1.1

Key: G_0 and G_{20} are non-PEGylated and PEGylated NLC containing metformin whereas Glucophage® is marketed metformin formulation (reference sample).

mean C_{max} for the latter was 249.48 ± 1.08 µg/mL, the mean C_{max} for metformin-loaded non-PEGylated and PEGylated NLC formulations were respectively 398.69 ± 2.53 and 601.87 ± 1.92 µg/mL. Moreover, the T_{max} values for the reference sample, non-PEGylated and PEGylated NLC formulations were 1.1, 3.0 and 5.5 h, respectively.

The implication of the pharmacokinetics results obtained from this study is that plasma concentration of metformin obtained with the reference sample was not sustained compared with the developed formulations. Thus, in contrast to the rapid exponential decrease in the reference sample, metformin-loaded non-PEGylated and PEGylated NLC

formulations maintained a steady slow decrease or gradual clearance of drug throughout the study. The AUC is an important parameter for measuring bioavailability of drug from dosage forms since it represents the total integrated area under the blood concentration time profile, which represents the amount of drug reaching the systemic circulation [32]. By implication, there was enhancement in the circulation longevity of metformin in the developed NLC formulations, but the effect was highest with metformin-loaded PEGylated NLC. This alteration in both the drug uptake and decay or decrease in metformin concentration in the blood by the formulation could be attributed to an increase in the circulating half-life of metformin when administered as metformin-loaded PEGylated NLC. Thus, the reason for the positive gain in the pharmacokinetics of the metformin-loaded non-PEGylated NLC (batch G_0) and its contribution in enhancing the antidiabetic activity of metformin may be attributed to the excipients used in the formulation; but in addition to that, the PEGylated nature of batch G_{20} ensured improvement in the afore-mentioned properties of the formulation and further delayed the clearance of metformin from the blood circulation. The clinical implications of the above findings is that at therapeutic dose, the developed metformin-loaded PEGylated NLC would give fast and sustained antidiabetic effect with reduced dose and dosing frequency and subsequently would enhance dosage compliance by diabetic patients, consistent with previous report [32].

4. Conclusions

Both non-PEGylated and PEGylated capryol-based NLC formulations of metformin showed optimal characterization confirming the suitability and compatibility of metformin, PEG and the lipid matrices. The *in vitro* model in this present work has proven to predict the enhanced release of metformin from the PEGylated and non-PEGylated capryol-based NLC formulations than the market sample - Glucophage® and was confirmed by the *in vivo* glucose lowering study. PEGylated capryol-based NLC formulations loaded with metformin have higher and sustained release, and improved and prolonged antidiabetic activities, even at reduced doses, than the market product with immediate and then retarding antidiabetic activity. Metformin-loaded PEGylated capryol-based NLCs have sustained, time-dependent increasing anti-hyperglycemic activities, even at reduced doses while the metformin-loaded non-PEGylated capryol-based NLC showed time-dependent decrease in anti-hyperglycemic activity. Furthermore, the pharmacokinetic parameters (AUC, C_{max} and T_{max}) of the optimized system indicate that the PEGylated characteristics of the NLC significantly ($p < 0.05$) contributed to the circulation longevity of metformin in the blood. This study has shown that non-PEGylated as well as PEGylated capryol-based NLCs represents a promising approach for improved release, delivery, bioavailability of metformin, enhanced treatment of type 2 diabetes mellitus than commercial metformin, and even at reduced doses. Thus, PEGylated NLC would promote reduction of dose, dosing frequency, and side effects/dose-related adverse effects of metformin, which will culminate into improved patients' compliance. Therefore, the adopted technique of metformin delivery by PEGylated NLC may be a promising tool which would need further evaluations with the hope that it could potentially aid in surmounting the pharmacokinetic challenges of metformin.

Declarations

Author contribution statement

Kenechukwu, Franklin Chimaobi: Conceived and designed the experiments; Analyzed and interpreted the data; Contributed reagents, materials, analysis tools or data; Wrote the paper.

Isaac, God'spower Tochukwu; Nnamani, Daniel Okwudili: Performed the experiments; Analyzed and interpreted the data; Wrote the paper.

Momoh, Mumuni Audu; Attama, Anthony Amaechi: Contributed reagents, materials, analysis tools or data; Wrote the paper.

Funding statement

This research work received financial support from the Tertiary Education Trust Fund (TETFund) (Grant no. TETFUND/DR&D/CE/NRF/2019/STI/46/) by Government of Nigeria.

Data availability statement

The authors are unable or have chosen not to specify which data has been used.

Declaration of interests statement

The authors declare no conflict of interest.

Additional information

No additional information is available for this paper.

Acknowledgements

Dr. Franklin C. Kenechukwu wishes to acknowledge Phospholipid GmbH, Köln, Germany for generous provision of Phospholipon® 90H (P90H), Ph. Eur. Carl Roth GmbH + Co. KG Karlsruhe, Germany for the king gift of polyethylene glycol 4000 (PEG 4000) and beeswax as well as Gattefossé, Saint – Priest Cedex, France for supplying Capryol-PGE 860 used in this research.

References

[1] R. Dumitrescu, C. Mehedintu, I. Briceag, V.L. Purcărea, D. Hudita, Metformin-clinical pharmacology in PCOs, J. Med. Life 8 (2) (Jun. 2015) 187–192.
[2] M. Qushawy, Effect of the surfactant and liquid lipid type in the physico-chemical characteristics of beeswax-based nanostructured lipid carrier (NLC) of metformin, Pharm. Nanotechnol. (Feb. 2021).
[3] G.G. Graham, et al., Clinical pharmacokinetics of metformin, Clin. Pharmacokinet. 50 (2) (Feb. 2011) 81–98.
[4] A.J. Scheen, Clinical pharmacokinetics of metformin, Clin. Pharmacokinet. 30 (5) (May 1996) 359–371.
[5] M. Momoh, M. Adedokun, M. Adikwu, F. Kenechukwu, E. Ibezim, E. Ugwuoke, Design, characterization and evaluation of PEGylated-mucin for oral delivery of metformin hydrochloride, Afr. J. Pharm. Pharmacol. 7 (7) (Feb. 2013) 347–355.
[6] M. Asadujjaman, A.U. Mishuk, Novel approaches in lipid based drug delivery systems, J. Drug Deliv. Therapeut. 3 (4) (Jul. 2013). Art. no. 4.
[7] M.A. Iqbal, S. Md, J.K. Sahni, S. Baboota, S. Dang, J. Ali, Nanostructured lipid carriers system: recent advances in drug delivery, J. Drug Target. 20 (10) (Dec. 2012) 813–830.
[8] N. K. Jain and A. Ram, "Development and characterization of nanostructured lipid carriers of oral hypoglycemic agent: Selection of Surfactants," vol. 7, no. 2, p. 6.
[9] S.-D. Li, L. Huang, Pharmacokinetics and biodistribution of nanoparticles, Mol. Pharm. 5 (4) (Aug. 2008) 496–504.
[10] E. Mun, B. Zhaisanbayeva, The role of nanoparticle PEGylation in drug delivery, Adv. Mater. Technol. (Jan. 2020) 10–18.
[11] M. Momoh, M. Adedokun, M. Adikwu, C. Ibezim, *In vitro* evaluation of PEGylated-mucin matrix as carrier for oral delivery of metformin hydrochloride, Trop. J. Pharmaceut. Res. 13 (7) (Sep. 2014) 1039.
[12] GlaxoSmithKline, The Effect of Food on the Pharmacokinetics of Metformin Given Either as Metformin Hydrochloride SR 1000 Mg Tablet or as a Fixed Dose Combination of Metformin Hydrochloride SR 1000mg/Glimepiride 2mg Tablet in Healthy Indian Volunteers., clinicaltrials.gov, Clinical trial registration NCT01561976, Sep. 2017. Accessed: Jul. 20, 2021. [Online]. Available: https://clinicaltrials.gov/ct2/show/NCT01561976.
[13] A. Dubey, P. Prabhu, Kamath, Nano Structured lipid carriers :A Novel Topical drug delivery system, Int. J. PharmTech Res. 4 (2) (Jun. 2012) 705–714.
[14] P.O. Nnamani, et al., Sustained-release liquisolid compact tablets containing artemether–lumefantrine as alternate-day regimen for malaria treatment to improve patient compliance, Int. J. Nanomed. 11 (Nov. 2016) 6365–6378.
[15] F. Shi, Z. Wei, Y. Zhao, X. Xu, Nanostructured lipid carriers loaded with baicalin: an efficient carrier for enhanced antidiabetic effects, Phcog. Mag. 12 (47) (2016) 198–202.
[16] R. Tiwari, K. Pathak, Nanostructured lipid carrier versus solid lipid nanoparticles of simvastatin: comparative analysis of characteristics, pharmacokinetics and tissue uptake, Int. J. Pharm. 415 (1–2) (Aug. 2011) 232–243.
[17] P.A. Akpa, et al., Improved antimalarial activity of caprol-based nanostructured lipid carriers encapsulating artemether-lumefantrine for oral administration, Afr. Health Sci. 20 (4) (Dec. 2020). Art. no. 4.

[18] U.K. Baruah, et al., Design, characterization and antimalarial efficacy of PEGylated galactosylated nano lipid carriers of primaquine phosphate, Artif. Cells Nanomed. Biotechnol. 46 (8) (Nov. 2018) 1809–1829.
[19] G. Shadambikar, et al., Formulation development of itraconazole PEGylated nano-lipid carriers for pulmonary aspergillosis using hot-melt extrusion technology, Int. J. Pharm. X 3 (Dec. 2021) 100074.
[20] S.P. Balguri, G.R. Adelli, K.Y. Janga, P. Bhagav, S. Majumdar, Ocular disposition of ciprofloxacin from topical, PEGylated nanostructured lipid carriers: effect of molecular weight and density of poly (ethylene) glycol, Int. J. Pharm. 529 (1) (Aug. 2017) 32–43.
[21] L. Wang, et al., PEGylated nanostructured lipid carriers (PEG–NLC) as a novel drug delivery system for biochanin A, Drug Dev. Ind. Pharm. 41 (7) (Jul. 2015) 1204–1212.
[22] X. Zhang, Y. Gan, L. Gan, S. Nie, W. Pan, PEGylated nanostructured lipid carriers loaded with 10-hydroxycamptothecin: an efficient carrier with enhanced anti-tumour effects against lung cancer, J. Pharm. Pharmacol. 60 (8) (2008) 1077–1087.
[23] X. Chen, et al., Preparation and evaluation of PEGylated asiatic acid nanostructured lipid carriers on anti-fibrosis effects, Drug Dev. Ind. Pharm. 46 (1) (Jan. 2020) 57–69.
[24] M.R.P. Rao, S. Aghav, G. Sukre, M. Kumar, Determination of required HLB of capryol 90, J. Dispersion Sci. Technol. 35 (2) (Feb. 2014) 161–167.
[25] A. Attama, et al., Solid lipid nanoparticles encapsulating a fluorescent marker (coumarin 6) and antimalarials - artemether and lumefantrine: evaluation of cellular uptake and antimalarial activity, Eur. J. Nanomed. 8 (3) (Jan. 2016) 129–138.
[26] N. Naseri, H. Valizadeh, P. Zakeri-Milani, Solid lipid nanoparticles and nanostructured lipid carriers: structure, preparation and application, Adv. Pharmaceut. Bull. 5 (3) (Sep. 2015) 305–313.
[27] M.A. Momoh, F.C. Kenechukwu, A.A. Attama, Formulation and evaluation of novel solid lipid microparticles as a sustained release system for the delivery of metformin hydrochloride, Drug Deliv 20 (3–4) (May 2013) 102–111.
[28] M. Zheng, M. Falkeborg, Y. Zheng, T. Yang, X. Xu, Formulation and characterization of nanostructured lipid carriers containing a mixed lipids core, Colloids Surf. A Physicochem. Eng. Asp. 430 (Aug. 2013) 76–84.
[29] F. Han, S. Li, R. Yin, H. Liu, L. Xu, Effect of surfactants on the formation and characterization of a new type of colloidal drug delivery system: nanostructured lipid carriers, Colloids Surf. A Physicochem. Eng. Asp. 315 (1) (Feb. 2008) 210–216.
[30] M. Jumaa, B.W. Müller, Influence of the non-ionic surfactant PEG-660-12-hydroxy stearate on the surface properties of phospholipid monolayers and their effect on lipid emulsion stability, Colloid Polym. Sci. 277 (4) (Apr. 1999) 347–353.
[31] C. Weingarten, N.S. Santos Magalhaes, A. Baszkin, S. Benita, M. Seiller, Interactions of a non-ionic ABA copolymer surfactant with phospholipid monolayers: possible relevance to emulsion stabilization, Int. J. Pharm. 75 (2) (Sep. 1991) 171–179.
[32] J.L. Perry, et al., PEGylated PRINT nanoparticles: the impact of PEG density on protein binding, macrophage association, biodistribution, and pharmacokinetics, Nano Lett 12 (10) (Oct. 2012) 5304–5310.
[33] G. S. Sanap and G. P. Mohanta, "Development of miconazile nitrate controlled release formulations based on SLN and NLC for tropicaal delivery," Int. J. Pharm. Pharmaceut. Sci., vol. 6, no. 4, pp. 393–399,[Online]. Available: https://innovareacademics.in/journal/ijpps/Vol6Issue4/9141.pdf.
[34] K. Abe, et al., Effects of the PEG molecular weight of a PEG-lipid and cholesterol on PEG chain flexibility on liposome surfaces, Colloids Surf. A Physicochem. Eng. Asp. 474 (Jun. 2015) 63–70.
[35] W. Li, P. Zhan, E. De Clercq, H. Lou, X. Liu, Current drug research on PEGylation with small molecular agents, Prog. Polym. Sci. 38 (3) (Mar. 2013) 421–444.
[36] F.M. Veronese, G. Pasut, PEGylation, successful approach to drug delivery, Drug Discov. Today 10 (21) (Nov. 2005) 1451–1458.
[37] X. Zhang, G. Chen, T. Zhang, Z. Ma, B. Wu, Effects of PEGylated lipid nanoparticles on the oral absorption of one BCS II drug: a mechanistic investigation, Int. J. Nanomed. 9 (Nov. 2014) 5503–5514.
[38] Y. Li, et al., In vivo delivery of BCNU from a MEMS device to a tumor model, J. Control. Release Off. J. Control. Release Soc. 106 (1–2) (Aug. 2005) 138–145.